Supplemental Figures belonging to:

Fusion of Intestinal Epithelial Cells with Bone Marrow Derived Cells is Dispensable for Tissue Homeostasis

Joan H. de Jong, Hans M. Rodermond, Cheryl D. Zimberlin, Valeria Lascano, Felipe De Sousa E Melo, Dick J. Richel, Jan Paul Medema and Louis Vermeulen

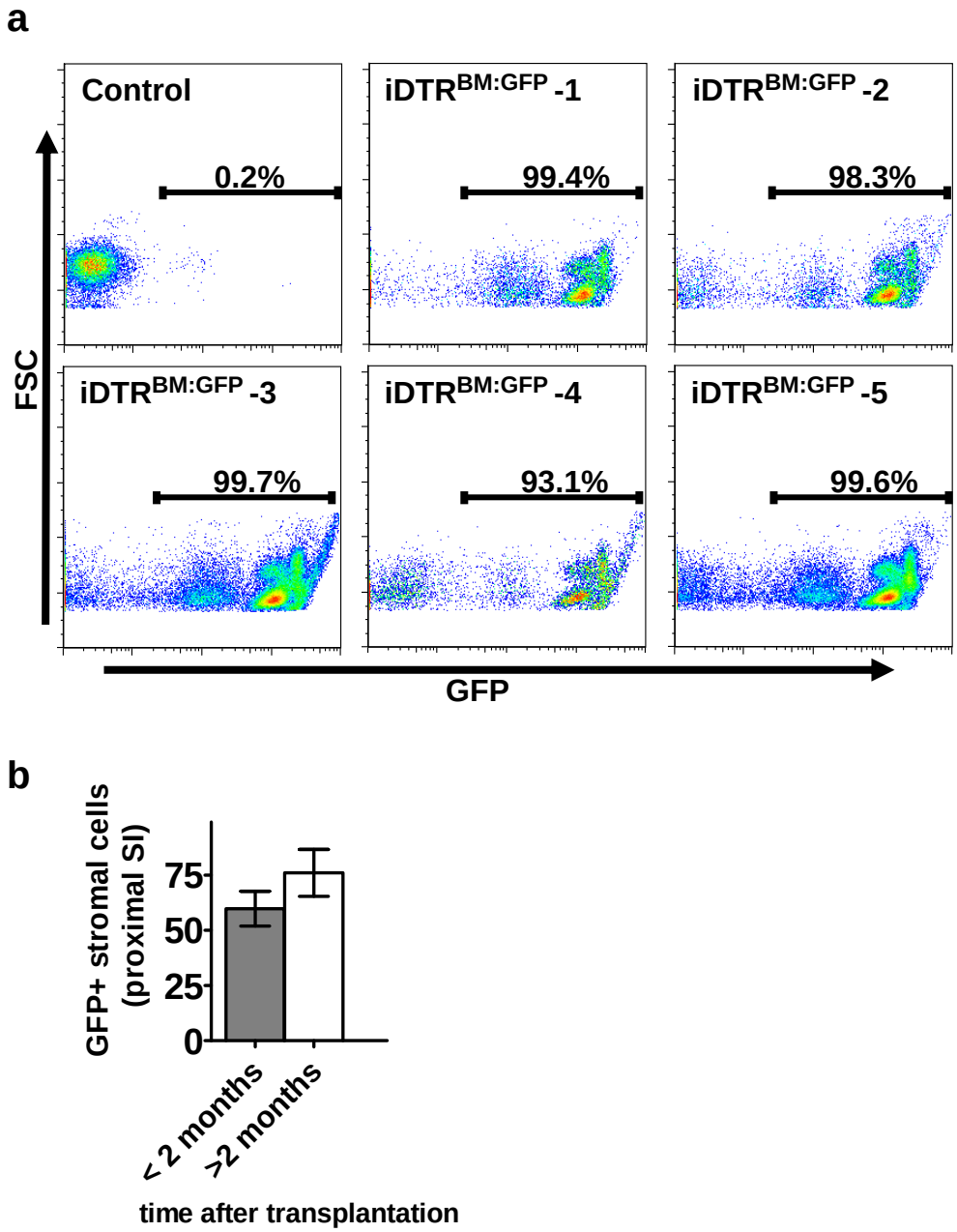

Figure S1 Efficient bone marrow engraftment following transplantation

(**A**) Evaluation of full blood of multiple iDTR$^{BM:GFP}$ mice confirms efficient bone marrow transplantation (6 weeks after transplantation). (**B**) Evaluation of intestinal stroma of iDTR$^{BM:GFP}$ mice reveals increasing extend of transplantation derived stromal cells with time. Error bars represent standard deviation, n=3 for both groups.

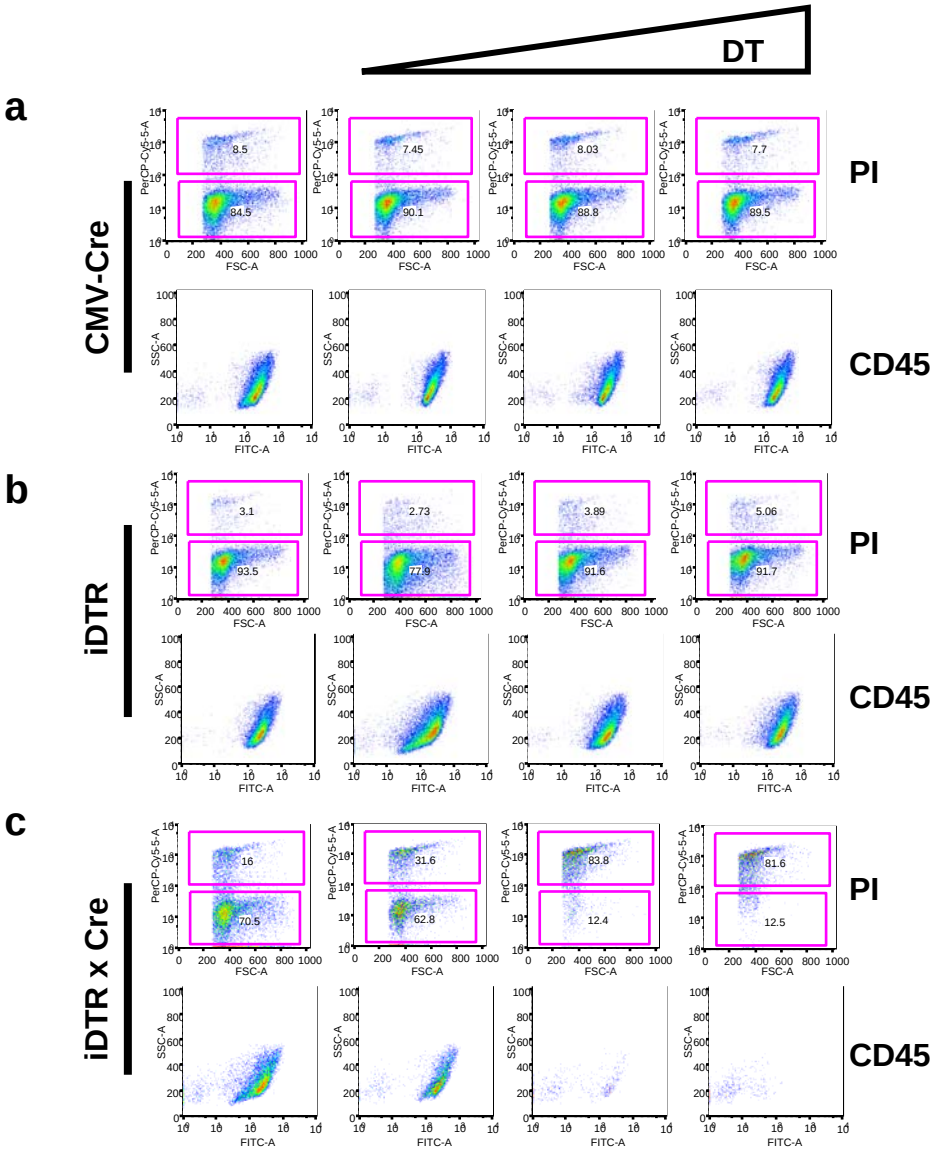

Figure S2 Efficient eradication of DTR expressing cells

(**A, B, C**) Splenocytes were isolated from CMV-Cre (**A**), iDTR (**B**), and iDTR x CMV-Cre (**C**) mice and cultured *in vitro* in DMEM supplemented with 25U/ml IL2 and 10% FCS. Cells were subsequently treated with increasing concentrations of DT (0, 0.01, 0.1, 1µg/ml) and evaluated for cell death, using propidium iodide (PI) after 24 hours. Marked cell death is observed in the DTR expressing cells from the iDTR x CMV-Cre mice (**C**).

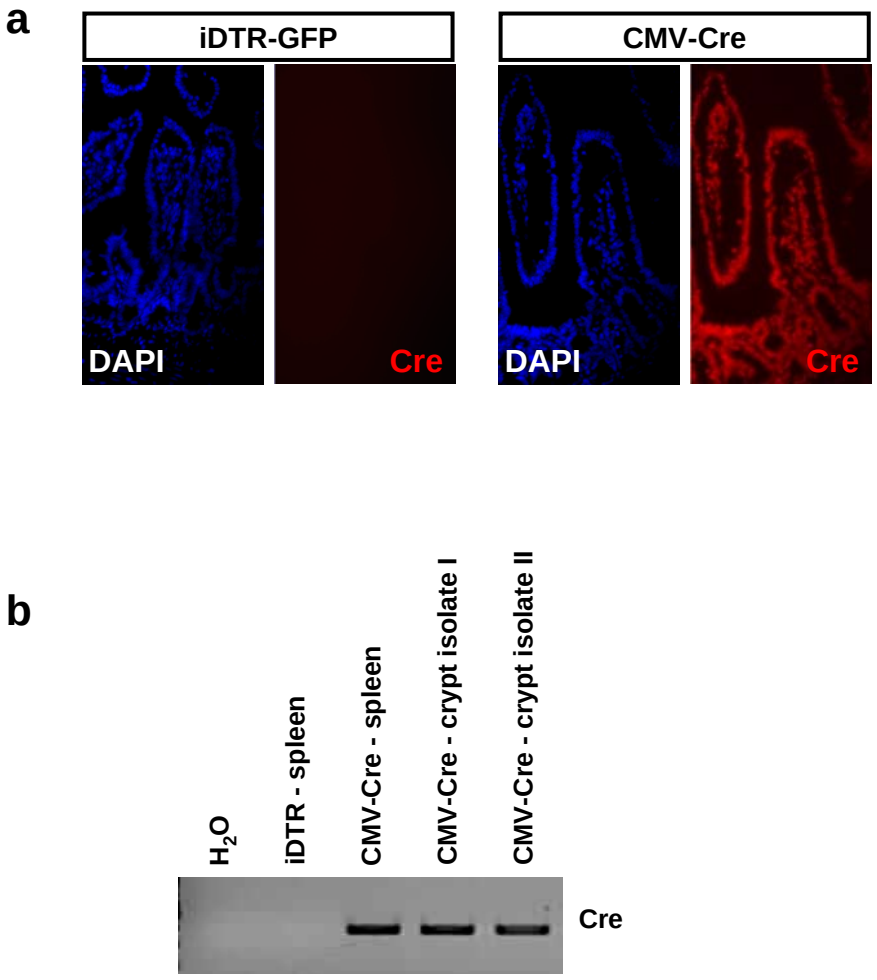

Figure S3 Cre is effectively expressed in intestinal epithelial cells in the CMV-Cre mouse (**A**) Immunostaining for Cre recombinase of small intestinal tissue derived from WT BL6 mice and CMV-Cre mice. (**B**) Evaluation of Cre expression by Cre PCR on RNA isolated from spleen iDTR mice (negative control) and CMV-Cre mice (positive control) as well as in isolated epithelial cells from the small intestine from CMV-Cre mice.

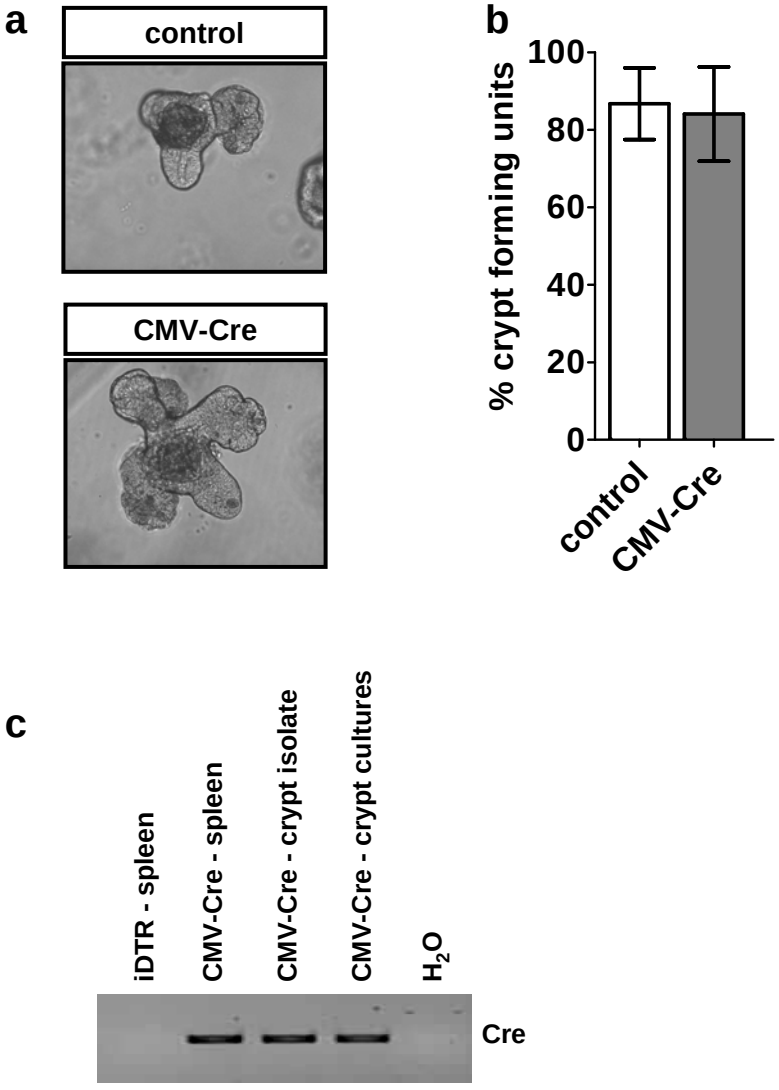

Figure S4 Cre expression does not impair intestinal stem cell function (**A**) Organoid cultures derived from CMV-Cre mice and control mice, 7 days after plating of small isolated crypt fragments. (**B**) Evaluation of budding organoid forming capacity of CMV-Cre mice demonstrates efficient organoid formation, at a level comparable to control mice (p=0.87). Small crypt fragments were plated and evaluated 7 days after plating. Error bars represent standard error of the mean. (**C**) Organoid structures from CMV-Cre mice retain Cre expression. Spleen cells and directly isolated crypt cultures from CMV-Cre mice are included as controls.

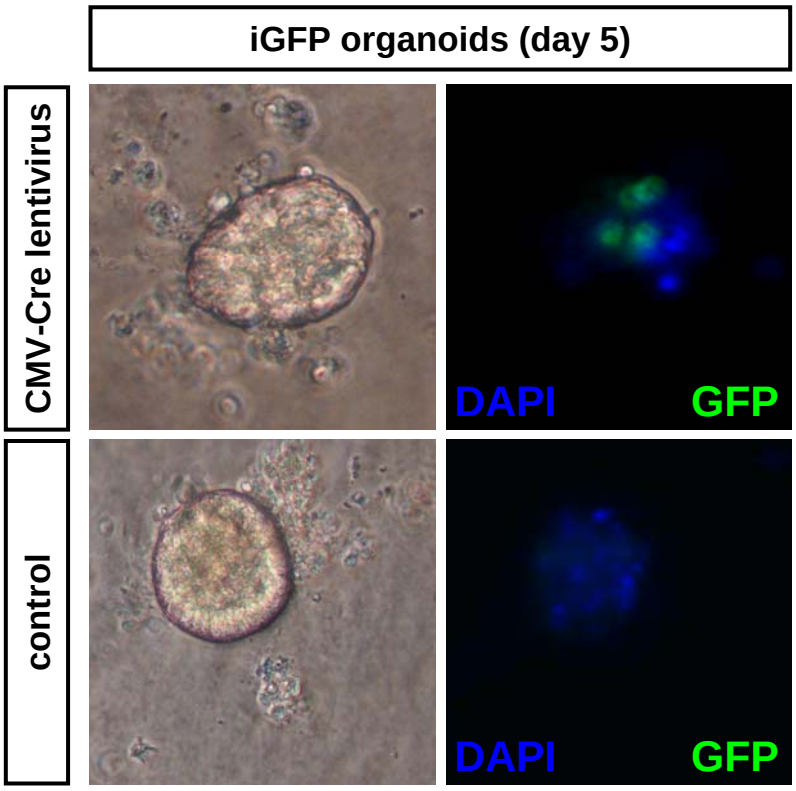

Figure S5 Recombination at the iGFP (Z/EG) locus effectively occurs in intestinal epithelial cells

Intestinal epithelial cells from iGFP mice were isolated and matrigel organoid cultures were initiated. At day 3 cultures were transduced with a lentiviral CMV-Cre vector. Two days after transduction GFP^+ cells start to emerge reflecting effective Cre mediated recombination at the iGFP (ZE/G) locus in intestinal epithelial cells.

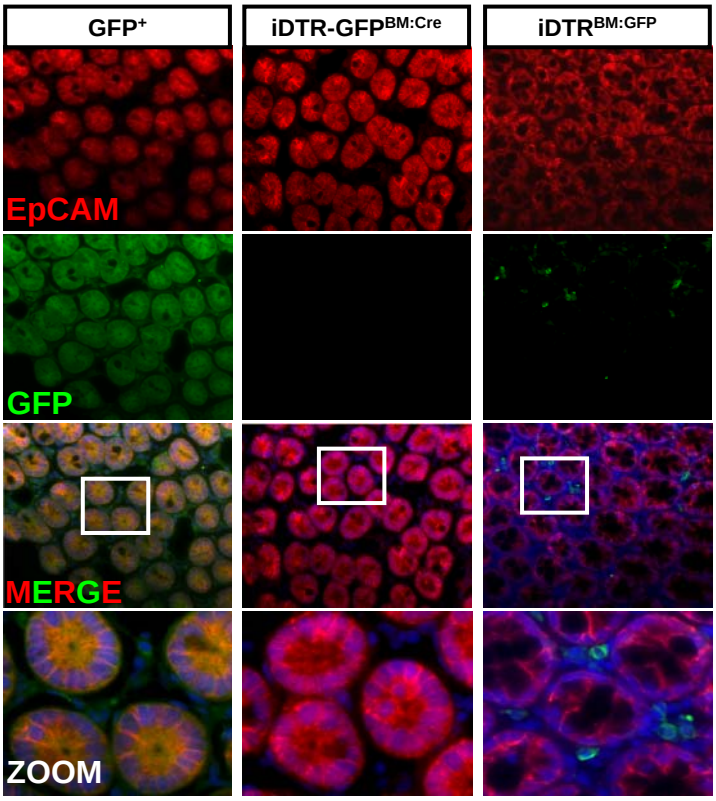

Figure S6 Immunofluorescence staining fails to detect fusion derived cells
Depicted are immunofluorescence stainings for GFP on the tissues indicated. No evidence for GFP expression in the epithelial compartment is detected.

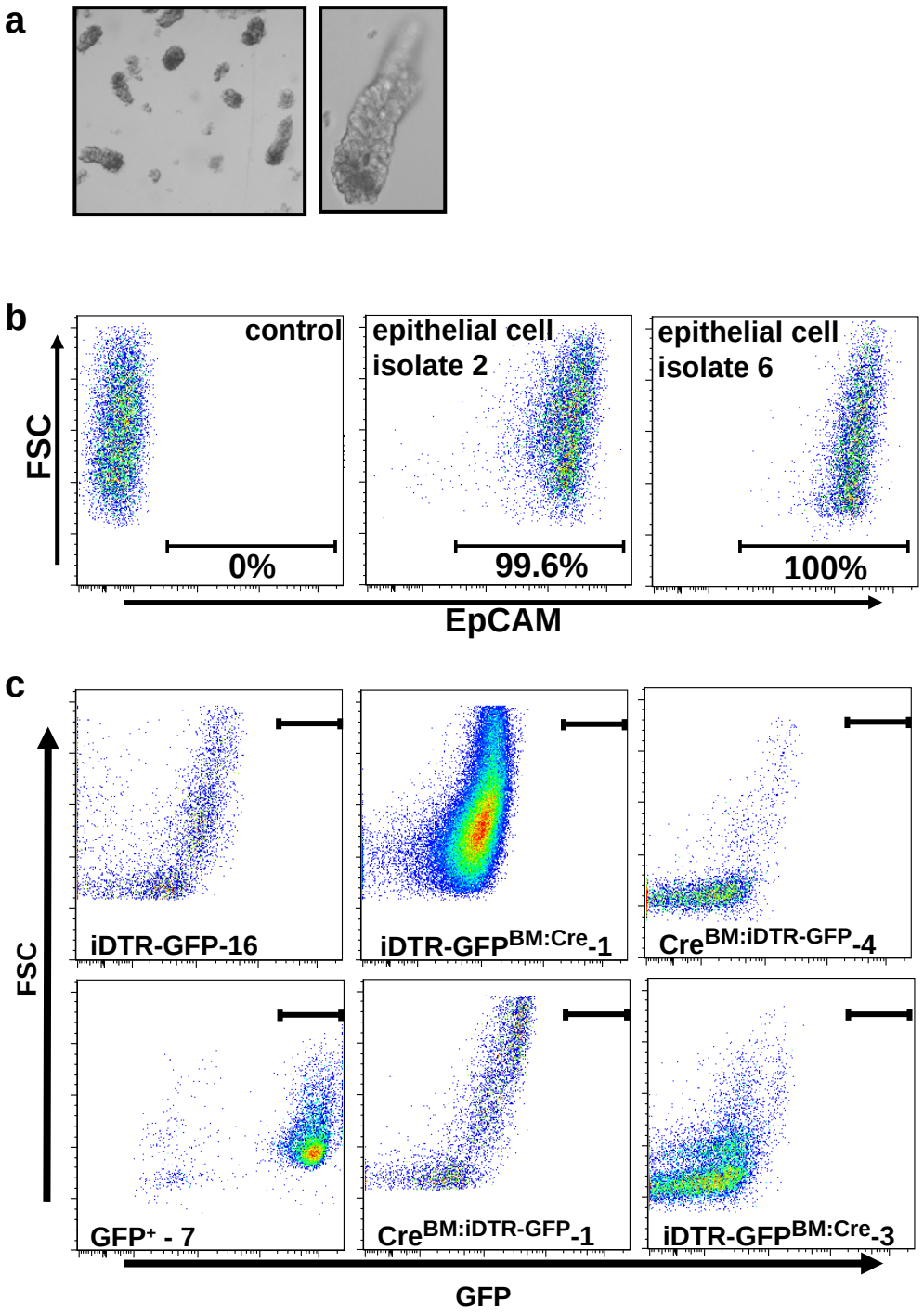

Figure S7 FACS analysis on epithelial isolates

(**A,B**) EDTA isolation of epithelial cell fraction of intestinal tissue generates pure epithelial cell fractions. (**C**) Multiple examples of lack of GFP detection in both iDTR-GFP$^{BM:Cre}$ and CMV-Cre$^{BM:iDTR-GFP}$ mice.

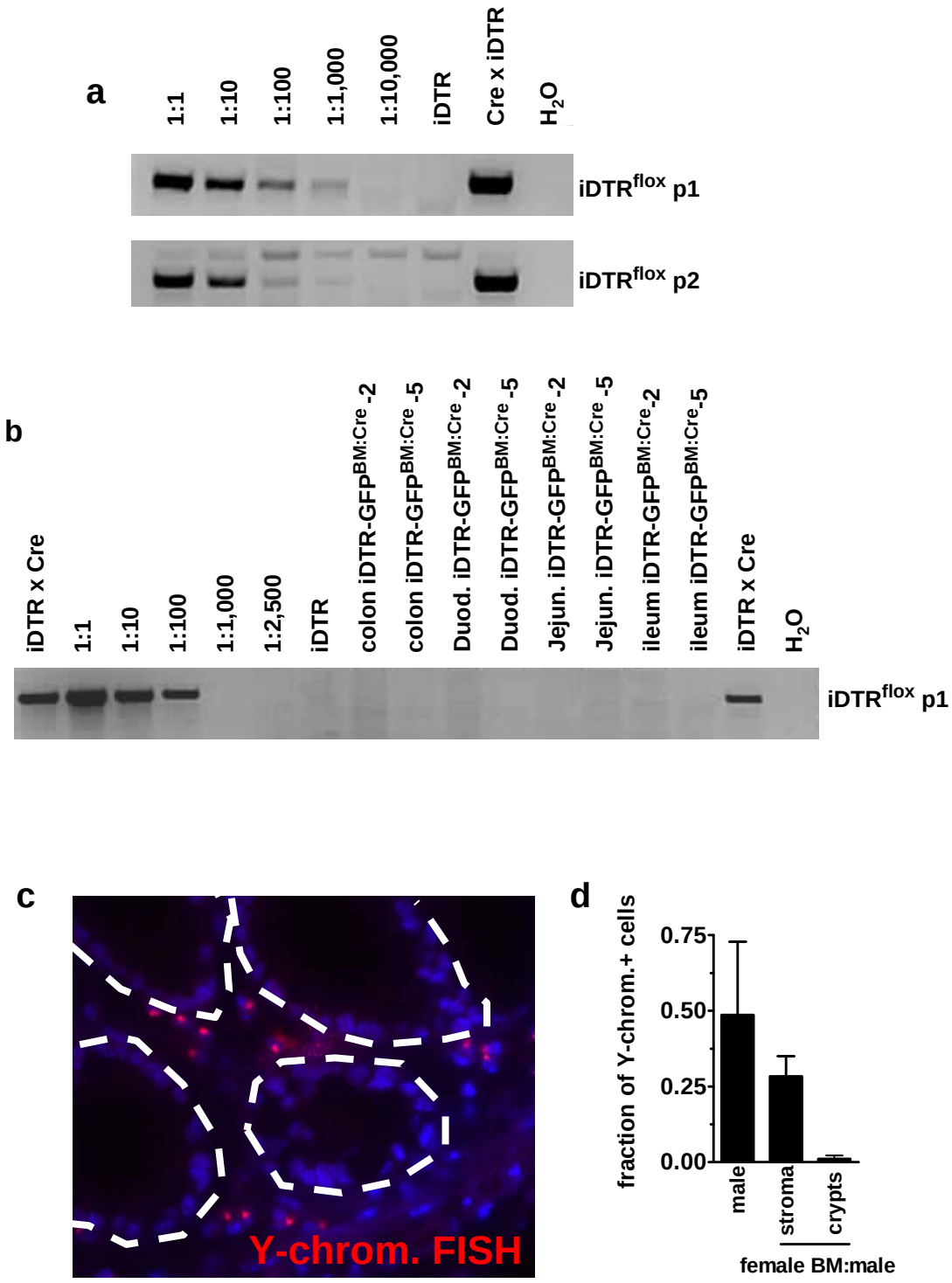

Figure S8

(**A**) Recombination specific PCR of the iDTR construct. A dilution series of genomic DNA from iDTR x CMV-Cre mice (containing recombined iDTR) in iDTR DNA is analyzed. Dilutions up to 1:1000 can be detected using this method. (**B**) DNA from isolated crypt structures in multiple intestinal sections are analyzed using the iDTR recombination specific PCR. No specific band could be detected indicating that recombination, signifying fusion events in iDTR-GFP$^{BM:Cre}$ mice, do not comprise more then 1 in every 1000 cells. (**C**) Fluorescence in situ hybridization (FISH) with Y-chromosome specific probes in female mice transplanted with male bone marrow. Clear Y-chromosome signal can be detected in the stroma compartment of these mice; only very sporadically a Y-chromosome positive nucleus is detected in the crypt structures. (**D**) Quantification of FISH analysis. Error bars represent standard deviation.

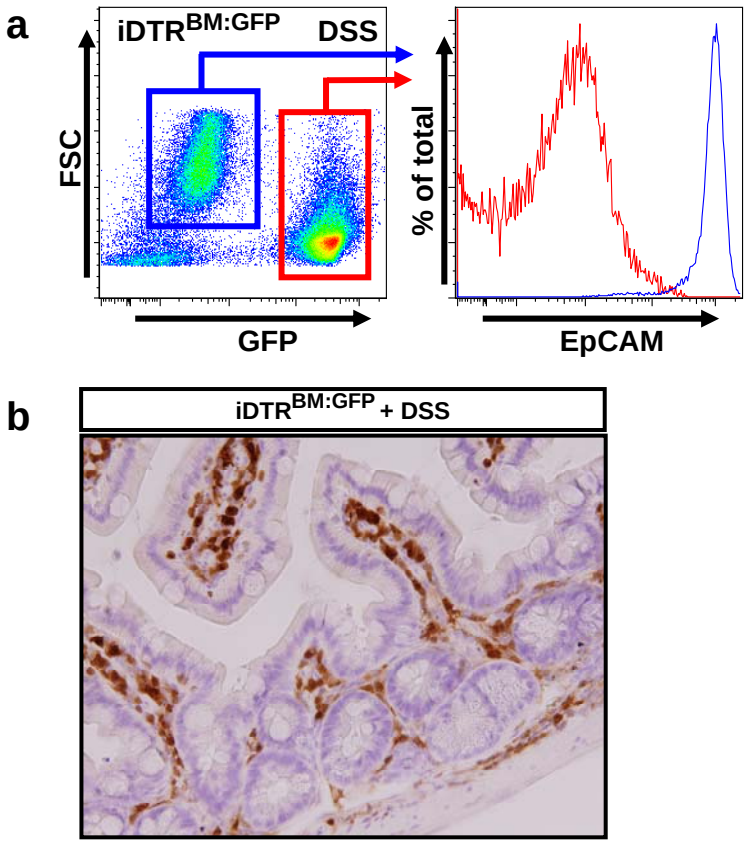

Figure S9 Inflammation does not promote cell fusion

(**A**) FACS analysis of DSS treated iDTR$^{BM:GFP}$ mice (as indicated in **Figure 4C**), reveals an extensive fraction of contaminating GFP^{+} cells. Much more then we detect in the intestines from non-DSS treated mice (e.g. **Figure 3, B** and **C**). However also in this setting we fail to detect EpCAM^{+} epithelial cells positive for GFP. (**B**) Extensive influx of GFP^{+} BMDCs can be detected also in the SI after DSS treatment of iDTR$^{BM:GFP}$ mice. No evidence could be obtained for segments of GFP^{+} epithelial cells (n=2).